Photochemistry of Solid Ozone

Arthur J. Sedlacek and Charles A. Wight*

Department of Chemistry, University of Utah, Salt Lake City, Utah 84112 *(Received: August 23, 1988)*

Samples of neat solid ozone and ozone trapped in excess ice have been subjected to laser photolysis at 308 nm. Cross sections for photoabsorption and photodestruction of the ozone are reported. The quantum yield decreases from 1.5 ± 0.2 in pure ozone to 0.4 ± 0.2 for ozone in excess ice. These yields are consistent with a reaction mechanism in which electronically excited $O(^1D)$ atoms are responsible for the photochemistry. In neat ozone, the atoms react with a neighboring ozone molecule to form two oxygen molecules. In water, $O(^1D)$ reacts to form hydrogen peroxide, HOOH. Ground-state oxygen atoms produced in the initial photolysis of ozone most likely undergo recombination with O_2 to regenerate O_3.

Introduction

Depletion of atmospheric ozone is a major environmental problem, especially in the polar regions.[1] Several studies have examined the photodissociation of ozone and subsequent reaction of the fragments with O_3,[2-11] H_2O,[12-23] and other small molecules.[24-31] However, the importance of ozone photochemistry in stratospheric ice crystals is largely unknown,[32,33] and to our knowledge no experimental investigation of this reaction in the solid state has been reported until now. The work of Vaida and co-workers[34-36] on the effects of intermolecular interactions on the electronic structure of simple molecules suggests that the photochemistry could be very different from that observed in the gas phase. This type of perturbative effect on the electronic spectrum of ozone is the subject of the accompanying paper.[37]

Here, we report cross sections for photodestruction of solid ozone (neat and in excess ice) at 308 nm, as well as measurements of the photoabsorption cross sections. The ratio of these is the photodestruction quantum yield, which decreases from 1.5 ± 0.2 in pure ozone to 0.4 ± 0.2 for ozone in excess ice. These results are discussed in terms of the reaction dynamics in an environment that severely restricts molecular motion.

Experimental Section

Details of the experimental apparatus and techniques are presented elsewhere.[38,39] Briefly, mixtures of gaseous reagents are deposited directly onto an optical window (quartz, CaF_2, or CsI) which is cooled to 10–77 K with a closed-cycle helium refrigerator. All of the results are temperature independent in this range. Ozone was prepared by electric discharge of oxygen, followed by distillation. Deposition rates were 3 μmol/min, and the total amount of ozone deposited was typically 30 μmol.

The photodestruction cross section was determined by measuring the UV absorbance (230–310 nm, Varian DMS-90 spectrometer) before and after irradiation with the 308-nm output of a XeCl excimer laser (Questek Model 2200). The laser fluence was 2.5 mJ/cm^2/pulse as measured with an absorbing disk calorimeter (Scientech Model 38-01). In some experiments, infrared absorption spectra of the samples were obtained with a Digilab Model FTS-40 infrared spectrometer.

Results and Discussion

The photodestruction cross section was determined by plotting $\ln (A/A_0)$ vs total laser fluence (photons/cm^2), as shown in Figure 1 (inset). For optically thin samples, the slope of this linear plot is equal to $-\sigma_d$. Absorbance at 308 nm was typically 0.1. Analysis

(1) Molina, M. J.; Tso, T.-L.; Molina, L. T.; Wang, F. C.-Y. *Science* **1987**, *238*, 1253. For papers on the subject, also see: *Geophys. Res. Lett.* **1986**, *13*, 45.
(2) Valentini, J. J. *J. Chem. Phys.* **1987**, *86*, 6759.
(3) Wine, P. H.; Nicovich, J. M.; Thompson, R. J.; Ravishankara, A. R. *J. Phys. Chem.* **1983**, *87*, 3948, and references therein.
(4) Cobos, C.; Castellano, E.; Schumacher, H. J. *J. Photochem.* **1983**, *21*, 291.
(5) Arnold, I.; Comes, F. J. *Chem. Phys.* **1980**, *47*, 125. Arnold, I.; Comes, F. J. *J. Mol. Struct.* **1980**, *61*, 223.
(6) Findlay, F. D.; Snelling, D. R. *J. Chem. Phys.* **1971**, *54*, 2750.
(7) Jones, I. T. N.; Wayne, R. P. *Proc. R. Soc. London* **1970**, *A319*, 273.
(8) Clark, I. D.; Jones, I. T. N.; Wayne, R. P. *Proc. R. Soc. London* **1970**, *A317*, 407.
(9) Norrish, R. G. W., F. R. S.; Wayne, R. P. *Proc. R. Soc. London* **1965**, *A288*, 200.
(10) Benson, S. D.; Axworthy, A. E., Jr. *J. Chem. Phys.* **1957**, *26*, 1718.
(11) McGrath, W. D.; Norrish, R. G. W., F. R. S. *Proc. R. Soc. London* **1959**, *A254*, 317.
(12) Lissi, E.; Heicklen, J. *J. Photochem.* **1972**, *1*, 39.
(13) Burrows, J. P.; Cox, R. A.; Derwent, R. G. *J. Photochem.* **1981**, *16*, 147.
(14) Butler, J. E.; Talley, L. D.; Smith, G. K.; Lin, M. C. *J. Chem. Phys.* **1981**, *74*, 4501.
(15) DeMore, W. B.; Tschvikow-Roux, E. *J. Phys. Chem.* **1974**, *78*, 1447.
(16) Langley, K. F.; McGrath, W. D. *Planet. Space Sci.* **1971**, *19*, 413.
(17) DeMore, W. D. *J. Chem. Phys.* **1967**, *46*, 2777.
(18) Norrish, R. G. W., F. R. S.; Wayne, R. P. *Proc. R. Soc. London* **1965**, *A288*, 361.
(19) Taube, H. *Trans. Faraday Soc.* **1957**, *53*, 656.
(20) Kilpatrick, M. L.; Herrick, C. C.; Kilpatrick, M. *J. Am. Chem. Soc.* **1956**, *78*, 1784.
(21) Alder, M. G.; Hill, G. R. *J. Am. Chem. Soc.* **1950**, *72*, 1884.
(22) Forbes, G. S.; Heidt, L. J. *J. Am. Chem. Soc.* **1934**, *56*, 1671.
(23) McGrath, W. D.; Norrish, R. G. W., F. R. S. *Nature* **1958**, *182*, 235.
(24) Aminoto, S. T.; Force, A. P.; Gulotty, R. G., Jr.; Wiesenfeld, J. R. *J. Chem. Phys.* **1979**, *71*, 3640.
(25) Wiesenfeld, J. R. *Acc. Chem. Res.* **1982**, *15*, 110.
(26) Whitten, R. C.; Prasad, S. S. *Ozone in the Free Atmosphere*; Van Nostrand Reinhold: New York, 1985.
(27) Schiff, H. I. *Ann. Geophys.* **1972**, *77*, 67.
(28) Aker, P. M.; Sloan, J. J. *J. Chem. Phys.* **1986**, *85*, 1412.
(29) Butler, J. E.; Jurisch, G. M.; Watson, I. A.; Wiesenfeld, J. R. *J. Chem. Phys.* **1986**, *84*, 5365.
(30) Aker, P. M.; O'Brien, J. J. A.; Sloan, J. J. *J. Chem. Phys.* **1985**, *84*, 745.
(31) Butler, J. E.; McDonald, R. G.; Donaldson, D. J.; Sloan, J. J. *Chem. Phys. Lett.* **1983**, *95*, 183.
(32) Crutzen, P. J.; Arnold, F. *Nature* **1986**, *324*, 651.
(33) McElroy, M. G.; Salawitch, R. J.; Wofsy, S. C. *Geophys. Res. Lett.* **1986**, *13*, 1296. Toon, O. B.; Hamill, P.; Turco, R. P.; Pinto, J. *Ibid.* **1986**, *13*, 1284. Hamill, P.; Toon, O. B.; Turco, R. P. *Ibid.* **1986**, *13*, 1288.
(34) Donaldson, D. J.; Vaida, V.; Naaman, R. *J. Phys. Chem.* **1988**, *92*, 1204. Donaldson, D. J.; Vaida, V.; Naaman, R. *J. Chem. Phys.* **1987**, *87*, 2522.
(35) Sapers, S. P.; Vaida, V.; Naaman, R. *J. Chem. Phys.* **1988**, *88*, 3638.
(36) Donaldson, D. J.; Gaines, G. A.; Vaida, V. *J. Phys. Chem.* **1988**, *92*, 2766.
(37) Vaida, V.; Donaldson, D. J.; Strickler, S.; Stephens, S.; Burks, J. W. *J. Phys. Chem.*, preceding paper in this issue.
(38) Sedlacek, A. J.; Manseuto, E. S.; Wight, C. A. *J. Am. Chem. Soc.* **1987**, *109*, 6223.
(39) Manseuto, E. S.; Ju, C.-Y.; Wight, C. A. *J. Phys. Chem.*, in press.

0022-3654/89/2093-0509$01.50/0 © 1989 American Chemical Society

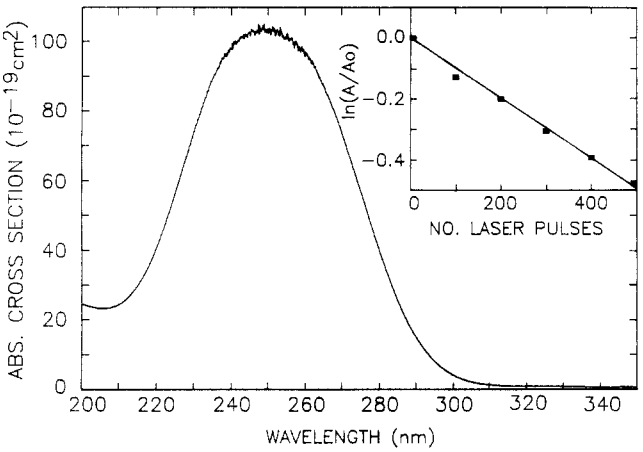

Figure 1. Absorption cross section (base e) as a function of wavelength for neat solid ozone at 10 K. The inset is a plot of ozone absorbance (at 270 nm) vs the number of laser pulses (fluence = 4.0×10^{15} photons/cm^2/pulse). The photodestruction cross section is obtained from the slope of this plot (see text for details).

of photochemical measurements in strongly absorbing media is the subject of a recent paper.[40]

Light scattering by some samples made it difficult to accurately determine the absorbance base line. These cross sections were evaluated by using a modified Guggenheim method[41]

$$\alpha_\phi = \alpha_{\phi+\Delta\phi} \exp(\sigma_d \Delta\phi) + \alpha_\infty(1 - \exp(\sigma_d \Delta\phi)) \quad (1)$$

where α_ϕ and $\alpha_{\phi+\Delta\phi}$ are the absorbances at fluences of ϕ and $\phi + \Delta\phi$, respectively, and α_∞ is the absorbance base line. Both types of data analysis yielded consistent values of σ_d. It should be noted that while light scattering sometimes influenced the absorbance measurements at short wavelengths (230–270 nm) it did not significantly affect the amount of light absorbed at the photolysis wavelength (308 nm). This was confirmed by direct measurements of the incident and transmitted laser beam intensities. For pure ozone samples $\sigma_d = (2.43 \pm 0.05) \times 10^{-19}$ cm^2 (four experiments). For ozone in excess ice ($H_2O:O_3$ = 10–50) $\sigma_d = (1.8 \pm 0.4) \times 10^{-19}$ cm^2 (five experiments). All uncertainties are quoted as 95% confidence limits. Cross sections are base e.

In each experiment, the photoabsorption cross section at 308 nm was determined by measuring the absorbance at that wavelength. For experiments in which light scattering was significant, the absorbance base line, α_∞, was determined from the intercept of the Guggenheim plot. In the calculation of σ_a from the measured absorbance, we assume that 11% of the total sample is deposited in 1 cm^2 at the center of the cold window. This value is based on the geometry of the deposition tube and window[38] and has been confirmed by other experiments.[39] Nevertheless, it represents a major source of uncertainty in the determination of σ_a. For pure solid ozone at 308 nm $\sigma_a = (1.7 \pm 0.2) \times 10^{-19}$ cm^2. This is essentially the same as the gas-phase value reported by Davenport,[42] $(1.51 \pm 0.21) \times 10^{-19}$ cm^2.

For ozone in excess ice, partial decomposition of the ozone occurred in the vacuum manifold during deposition. The actual amount of sample deposited was determined by measuring the integrated IR band intensities at 1090 and 2104 cm^{-1}. These were compared with a sample of pure ozone deposited under conditions where decomposition was negligible. The IR bands of ozone are not strongly affected by the presence of H_2O, as shown by the invariance of the relative intensities of the two IR bands under all experimental conditions we have investigated thus far. The 308-nm photoabsorption cross section for ozone in excess ice was determined to be $\sigma_a = (4.0 \pm 1.9) \times 10^{-19}$ cm^2.

TABLE I: Relevant State-Specific Reactions of Ozone and Water[a]

reaction	ΔH, kcal/mol	
$O(^3P) + O_3(^1A) \rightarrow 2O_2(^3\Sigma_g^-)$	−92.2	SA
$O(^1D) + O_3(^1A) \rightarrow 2O_2(^3\Sigma_g^-)$	−137.4	SA
$O_2(^3\Sigma_g^-) + O_3(^1A) \rightarrow 2O_2(^3\Sigma_g^-) + O(^3P)$	25.0	SA
$O_2(^1\Delta_g) + O_3(^1A) \rightarrow 2O_2(^3\Sigma_g^-) + O(^3P)$	2.9	SA
$O_2(^1\Sigma_g^+) + O_3(^1A) \rightarrow 2O_2(^3\Sigma_g^-) + O(^3P)$	−12.0	SA
$O(^3P) + H_2O(^1A) \rightarrow HOOH(^1A)$	−32.9	SF
$O(^1D) + H_2O(^1A) \rightarrow HOOH(^1A)$	−77.7	SA
$O(^3P) + H_2O(^1A) \rightarrow 2OH(^2\Pi)$	16.8	SA
$O(^1D) + H_2O(^1A) \rightarrow 2OH(^2\Pi)$	−29.2	SA

[a] SF = spin forbidden and SA = spin allowed.

TABLE II: Primary Photolysis Channels for Ozone in Visible and UV

photolysis channel	wavelength threshold, nm
$O_3(^1A) \rightarrow O_2(^3\Sigma_g^-) + O(^3P)$	1180
$\rightarrow O_2(^1\Delta_g) + O(^3P)$	611
$\rightarrow O_2(^1\Sigma_g^+) + O(^3P)$	463
$\rightarrow O_2(^3\Sigma_g^-) + O(^1D)$	411
$\rightarrow O_2(^1\Delta_g) + O(^1D)$	310
$\rightarrow O_2(^1\Sigma_g^+) + O(^1D)$	266

The ratio of the photodestruction and photoabsorption cross sections is the photochemical quantum yield (number of ozone molecules destroyed per photon absorbed by the sample). In pure ozone the quantum yield is 1.5 ± 0.2 whereas in excess ice it decreases to 0.4 ± 0.2. In the gas phase,[12] the photochemical quantum yield of pure ozone is nearly 6. In the presence of excess water vapor it increases to a limiting value of 17. In the following discussion, we speculate on some of the reasons for the smaller quantum yields observed in the solid as compared with the gas phase.

Primary photolysis of gas phase ozone at 308 nm is believed to occur by two spin-allowed channels, reactions 2 and 3,[27] where

$$O_3 \xrightarrow{h\nu} \xrightarrow{I_{abs}(1-\phi)} O(^3P) + O_2(^3\Sigma_g^-) \quad (2)$$

$$O_3 \xrightarrow{h\nu} \xrightarrow{I_{abs}\phi} O(^1D) + O_2(^1\Delta_g) \quad (3)$$

ϕ is the quantum yield for $O(^1D)$ formation. The oxygen atom may react with another molecule of ozone to form two oxygen molecules. In the solid state, we postulate that only $O(^1D)$ atoms react with neighboring ozone molecules. The most likely fate of the $O(^3P)$ atoms is recombination with O_2 to form ozone.

$$O(^1D) + O_3 \rightarrow 2O_2 \quad (4)$$

$$O(^3P) + O_2 \rightarrow O_3 \quad (5)$$

We further postulate that electronically excited O_2 molecules do not contribute to the destruction of ozone in the solid state. Table I shows that the reaction of $O_2(^1\Sigma_g^+)$ is exothermic, but this species can only be produced at 308 nm via a spin-forbidden process forming $O(^3P)$, as shown in Table II.

McGrath and Norrish[23] have reported evidence that the reaction of $O(^1D)$ with O_3 produces a vibrationally excited O_2 molecule with sufficient energy to further react with another O_3 and regenerate $O(^1D)$. However, vibrational deactivation of O_2 in the solid state should rapidly lower its energy to below the reaction threshold (v = 17), rendering the O_2 molecule unreactive.

If the reaction scheme outlined above is correct, then we should observe a quantum yield for photodestruction of ozone which is twice the quantum yield for production of $O(^1D)$ in the primary step. This is because $O(^3P)$ is assumed to undergo recombination (no net reaction) while $O(^1D)$ atoms each destroy a second O_3 molecule in reaction 4. The primary $O(^1D)$ yield is reported to be 0.79 ± 0.2 in the gas phase,[43–46] which is about half of our

(40) Sheats, J. R.; Diamond, J. J.; Smith, J. M. *J. Phys. Chem.* **1988**, *92*, 4922.

(41) Guggenheim, E. A. *Philos. Mag.* **1926**, *2*, 538. Also see: Moore, J. W.; Pearson, R. G. *Kinetics and Mechanism*, 3rd ed.; Wiley: New York, 1981.

(42) Davenport, J. E. Parameters for Ozone Photolysis as a Function of Temperature at 280–330 nm. Report No. FAA-EE-80-44, Contract No. DOT-FA78WA-4263.

(43) Arnold, I.; Comes, F. J.; Moortgat, G. K. *Chem. Phys.* **1977**, *24*, 21.

measured photodestruction yield of 1.5 ± 0.2 in the solid state. This lends support to the proposed reaction mechanism.

When ozone is trapped in excess ice, the measured photodestruction quantum yield is 0.4 ± 0.2. Reaction of $O(^3P)$ with H_2O to form hydrogen peroxide is exothermic, but spin forbidden. $O(^1D)$ atoms can form HOOH or two OH radicals. In the solid state we expect that either mechanism would lead to the stabilization and/or formation of HOOH due to radical recombination in the reaction cavity.[47] If we again make the hypothesis that

$$O(^1D) + H_2O \rightarrow HOOH \quad (6)$$

$O(^3P)$ atoms undergo recombination with their partner O_2 molecules and only the channels producing $O(^1D)$ atoms are responsible for the net destruction of ozone, we predict that the photodestruction quantum yield should be equal to the quantum yield for $O(^1D)$ formation in the primary step. Few direct measurements of this quantity are available. Taube[19] has reported the $O(^1D)$ quantum yield of ozone in liquid water to be 0.21 at 313 nm, so our value of 0.4 ± 0.2 at 308 nm is not unreasonable agreement.

We have observed IR absorption bands in the photolyzed O_3/H_2O samples at 1405 and 2860 cm^{-1} which are attributable to HOOH reaction product.[48] These bands shift to 1075 and 2130 cm^{-1} when the experiment is carried out with D_2O, a result which is consistent with formation of DOOD. It is worth noting that, in the gas phase, reaction of $O(^1D)$ with H_2O produces two OH radicals. These are chain reaction carriers which make the overall quantum yield for ozone destruction quite high. In the solid state, however, the HOOH molecule is stabilized as a final product. No chain reaction occurs, and the overall quantum yield for photodestruction of O_3 is low.

The experimental results suggest that the photolysis of O_3 in stratospheric polar ice crystals is not an efficient mechanism for ozone destruction because the solid itself inhibits the formation of OH chain reaction carriers. In addition, the antarctic atmosphere has a sharp wavelength cutoff at 310 nm, which is the threshold wavelength for producing $O(^1D)$ atoms from ozone via spin-allowed reactions (Table II). This may also limit the extent of ozone photochemistry since our results suggest that $O(^3P)$ atoms undergo recombination to re-form O_3. Consequently, the direct photodissociation of ozone in ice crystals is not likely to make a significant contribution to the overall observed depletion of atmospheric ozone.

Experiments are now under way to elucidate the dependence of the photodestruction quantum yield on the relative concentrations of ozone and water in the solid samples. We are also investigating the wavelength dependence of the photochemistry to gain additional information about the electronic-state selectivity of reactions in the solid.

Acknowledgment. We thank Professors D. J. Donaldson and Veronica Vaida for helpful discussions and Professor John Spikes for the loan of the UV absorption spectrometer. This research was supported by the U.S. Air Force Astronautics Laboratory (Contract No. F04611-87-K-0023).

(44) Brock, J. C.; Watson, R. T. *Chem. Phys.* **1980**, *46*, 477.
(45) Moortgat, G. K.; Kudszus, E. *Geophys. Res. Lett.* **1978**, *5*, 191.
(46) Steinfeld, J. I.; Alder-Golden, S. M.; Gallagher, J. W. JILA Data Center Report No. 31, JILA, University of Colorado, 1987.
(47) Cohen, M. D. *Angew. Chem., Int. Ed. Engl.* **1975**, *14*, 386.
(48) Bain, O.; Giguere, P. A. *Can. J. Chem.* **1954**, *33*, 527.

Scanning Tunneling Microscopic Imaging of Electropolymerized, Doped Polypyrrole. Visual Evidence of Semicrystalline and Helical Nascent Polymer Growth

R. Yang, K. M. Dalsin, D. F. Evans,

Department of Chemical Engineering and Materials Science, University of Minnesota, Minneapolis, Minnesota 55455

L. Christensen, and W. A. Hendrickson*

3M Company, Corporate Research Laboratory, 3M Center, St. Paul, Minnesota 55144
(Received: November 8, 1988)

We have examined electropolymerized polypyrroles doped with *p*-toluenesulfonate (TOS), tetrafluoroborate (TFB), or trifluoroacetate (TFA), using scanning tunneling microscopy (STM). The initial stages of polymer growth involves microisland formation with concomitant polymer strands. In one case, the *p*-toluenesulfonate-doped polypyrrole, those strands have been shown to be helical.

Conducting polymers have been extensively investigated since the discovery in 1977 that doped polyacetylene was electrically conducting.[1] Polypyrrole is a particularly attractive material for commercial application because of its ease of formation[2] and relative stability in the doped, conductive form.[3] Its physical properties depend on the dopant anion incorporated into the polymer[4] as well as the conditions of polymer formation. However, the amorphous and insoluble nature of the polymer makes structural characterization difficult. NMR, IR, and XPS studies on solid, thick films established that the pyrrole units are predominately bonded through α-linkages.[5,6] X-ray diffraction analysis of 14–35-μm thick free-standing polypyrrole films shows that the polymers are macroscopically disordered and amorphous; however, the individual pyrrole units are coplanar with each other and are parallel to the original electrode surface.[7] However, X-ray and TEM studies on thin films show that they grow in several

* To whom correspondence should be addressed.

(1) Shirakawa, H.; Louis, E. J.; MacDiarmid, A. G.; Chiang, C. K.; Heeger, A. J. *J. Chem. Soc., Chem. Commun.* **1977**, 578.
(2) Street, G. B. In *Handbook of Conducting Polymers*; Skotheim, T. A., Marcel Dekker: New York, 1986; Vol. 1, Chapter 8.
(3) Billingham, N. C.; Calvert, P. D.; Foot, P. J. S.; Mohammad, F. *Polym. Degrad. Stab.* **1987**, *19*, 323.
(4) Reynolds, J. R. *CHEMTECH* **1988**, *18*(7), 440.
(5) Street, G. B.; Clarke, T. C.; Krounbi, M.; Kanazawa, K.; Lee, V.; Pfluger, P.; Scott, J. C.; Weiser, G. *Mol. Cryst. Liq. Cryst.* **1982**, *83*, 253–264.
(6) Zeller, M. V.; Hahn, S. J. *Surf. Interphase Anal.* **1988**, 327.
(7) Mitchell, G. R.; Geri, A. *J. Phys. D: Appl. Phys.* **1987**, *20*, 1346.

0022-3654/89/2093-0511$01.50/0 © 1989 American Chemical Society